

Rock topography causes spatial variation in the wave, current and beach response to sea breeze activity

Shari L. Gallop^{a,*}, Cyprien Bosserelle^a, Charitha Pattiaratchi^a, Ian Eliot^b

^a School of Environmental Systems Engineering and The UWA Oceans Institute, The University of Western Australia, 35 Stirling Highway, M015, Crawley, WA 6009, Australia

^b Damara WA Pty Ltd, PO Box 1299, Innaloo, WA 6018, WA, Australia

ARTICLE INFO

Article history:

Received 21 April 2011

Received in revised form 4 October 2011

Accepted 9 October 2011

Available online 18 October 2011

Communicated by J.T. Wells

Keywords:

perched beach
geological control
hard-bottom
rock platform
coastal structures
coastal lagoon

ABSTRACT

We hypothesized that beach profiles that are perched on natural rock structures would be better protected from waves and currents than profiles that are not fronted by rock. In southwest Western Australia many beaches, such as at Yanchep, are perched on Quaternary limestone. Yanchep Lagoon is fronted by a low-crested limestone reef that partially encloses a coastal lagoon. The spatial variation of waves and currents around the rock structures were quantified during the sea breeze cycle at locations: (1) offshore; (2) 20 m seaward of the reef; (3) inside the lagoon; and (4) in the surf zone. The spatial variation in the beach profile response was measured at two beach profiles: (1) the *Exposed Profile* that was not fronted directly seaward by outcropping limestone; and (2) the *Sheltered Profile* which was fronted seaward by submerged limestone at 2 m water depth and that was near the lagoon exit at the end of the limestone reef. The Sheltered Profile had greater volume changes during the cycle of the sea breeze whilst the Exposed Profile recovered more by overnight accretion when wind decreased. The lagoonal current drove the strong response of the Sheltered Profile and may have contributed to the lack of overnight recovery of the beach together with the seaward rock formation impeding onshore sediment transport. The different direction and speed responses of bottom-currents in the surf zone fronting the two profiles reflected the local variation in geology, the influence of the jet exiting the lagoon, and wave refraction around the reef that was measured with GPS drifters and wave-ray tracing using XBeach. Major spatial variation in waves, currents and beachface behavior at this perched beach shows the importance of the local geological setting.

© 2011 Elsevier B.V. All rights reserved.

1. Introduction

Beaches that have underlying rock and/or that are fronted seaward by geological or engineered structures are common world-wide. These beaches can be referred to as *perched beaches*, defined as being formed by the accumulation of unconsolidated sediment atop a shallow-rock platform; and/or that are landward of an offshore structure. Such structures may consist of limestone, coral, coquina, shell, worm rock, sedimentary rock, clay or rip-rap (Larson and Kraus, 2000). Internationally, different forms of perched beaches have been described including:

- (i) beaches with patchy exposed rock—often beach rock formed through the precipitation of carbonate sediments (Chowdhury et al., 1997; Dickinson, 1999; Rey et al., 2004; Vousdoukas et al., 2007, 2009);
- (ii) shore platforms (Bartrum, 1926; Muñoz-Pérez et al., 1999; Trenhaile, 2004; Valvo et al., 2006);

- (iii) inlets with a hard-bottom (Hanson and Militello, 2005);
- (iv) offshore breakwaters and reefs, possibly fronted landward by a coastal lagoon (Sanderson and Eliot, 1996; Dean et al., 1997; González et al., 1999; Eversole and Fletcher, 2003; Frihy et al., 2004); and
- (v) seawalls, revetments and bulkheads (Kraus, 1988; Fitzgerald et al., 1994; Kraus and McDougal, 1996).

In southwest Western Australia rocky beaches have been described by Semeniuk and Johnson (1982), Green (2008), Doucette (2009) and Da Silva (2010), and in the northwest beaches associated with coral such as the fringing reef at Ningaloo (Sanderson, 2000) are also an important part of the coast. A simple classification summarizing the above perched beach descriptions is presented in Fig. 1, focusing purely on the cross-shore perched beach profile rather than alongshore variations due to headlands and reefs which influence longshore sediment transport (Sanderson and Eliot, 1999). Perched beaches may also be backed by hard structures such as cliffs, seawalls, streets or buildings (Fitzgerald et al., 1994) which are not considered for the purpose of the simple classification.

The lack of research on perched beaches was mentioned by Hegge et al. (1996), who noted that while a morphodynamic classification of

* Corresponding author. Tel.: +61 8 6488 8117.

E-mail addresses: gallop@sese.uwa.edu.au (S.L. Gallop), bossere@sese.uwa.edu.au (C. Bosserelle), chari.pattiarachi@uwa.edu.au (C. Pattiaratchi), ian.eliot@bigpond.com (I. Eliot).

Perched Beach Classification

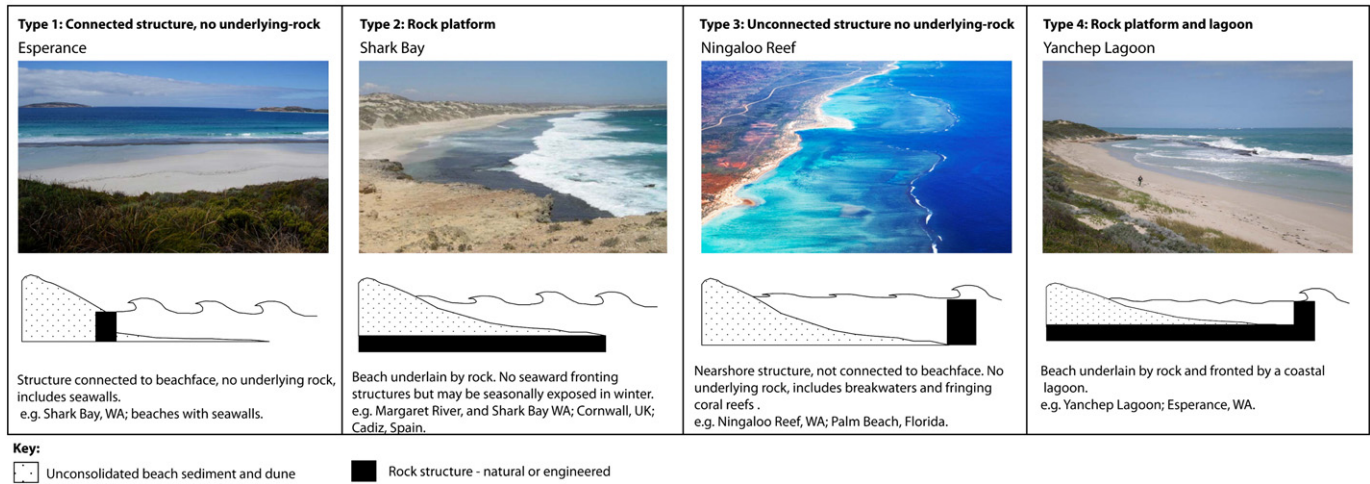


Fig. 1. A simple perched beach classification of the four main types, with Western Australian examples.

sandy beaches has been established for open-ocean, wave-dominated environments, many natural beaches are in fact inside embayments or landward of protective reefs which provide shelter from waves. It is accepted that the geology of perched beaches will affect the near-shore hydrodynamics and beach morphology, but there has been little research to quantify and understand these differences compared to 'typical' sandy beaches without structural constraints (Larson and Kraus, 2000; Stephenson and Thornton, 2005; Naylor et al., 2010). The response of shorelines to submerged structures such as artificial surfing reefs, is still poorly understood (Ranasinghe et al., 2006). With the threat of sea level rise and increased urbanization of the coast, understanding all types of coastal landforms is becoming more important so it is crucial that the mechanisms of geological beach control are identified.

It has been suggested that a rocky bottom at a beach will:

- (i) limit fluctuation of beach profiles (Larson and Kraus, 2000; Vousdoulas et al., 2007);
- (ii) alter the nearshore hydrodynamics (Cleary et al., 1996; Larson and Kraus, 2000; Vousdoulas et al., 2007);
- (iii) change the flow/ pressure distribution in the beach sediment (Larson and Kraus, 2000);
- (iv) reduce the porosity of the beach hence reduce water infiltration possibly leading to erosion (Walton and Sensabaugh, 1979; Larson and Kraus, 2000; Vousdoulas et al., 2009);
- (v) alter erosion rates at rock margins causing scouring (Larson and Kraus, 2000) by changing cross-shore and longshore sediment transport (Vousdoulas et al., 2007); and
- (vi) decrease sediment availability (Trenhaile, 2004) because if hard-bottom is exposed, the actual sediment transport rate will be less than the potential, which can also affect surrounding areas without hard-bottoms (Hanson and Militello, 2005).

In a study of the 10,685 mainland beaches of Australia, Short (2006) stressed the importance of geological formations to the form and function of perched beaches. It was noted that bedrock and calcarenite play a major role on Australian beaches by forming beach boundaries so that the average beach length is just 1.37 km. Australian rock formations lie along the coast as beachrock, rocks, headlands and islands, inducing wave refraction and attenuation resulting in lower energy beach types. Rocks were found to dominate the intertidal zone of 779 beaches, and coral reefs are located seaward of at least 1430 beaches in northern Australia. These are mostly barrier beaches that are backed by a lagoon with lower energy beaches that are unusually steep, most common in Western Australia.

Perched beaches are especially common in Western Australia. Yanchep Lagoon in the Perth metropolitan area of southwest Western Australia is predominantly a Type 4 (Fig. 1) perched beach that is partly fronted by a lagoon that is enclosed by a calcarenite limestone reef (Fig. 2). The microtidal coast is largely sheltered from swell by offshore reefs made of Quaternary limestone. Therefore, locally produced wind waves and currents from the unusually strong and persistent sea breeze that blows in summer have a dominant effect on coastal processes (Pattiaratchi et al., 1997), making the coast an ideal field location to quantify the response of beaches to wave and current forcing. The generally shore-parallel sea breeze in southwest Western Australia forms due to a combination of local and synoptic systems and plays a key role in the sediment budget of the coast by driving the mean annual littoral drift to the north (Masselink, 1996). The sea breeze increases significant wave height (H_s) at the coast by up to 0.9 m and can increase sediment suspension tenfold (Pattiaratchi et al., 1997). Past research on the effects of sea breeze activity on coastal processes and geomorphology in southwest Western Australia have focused mainly on beach cusps and have largely excluded the overnight recovery phase of beach morphology that occurs at the cessation of the sea breeze (Kempin, 1953; Pattiaratchi et al., 1997; Masselink and Pattiaratchi, 1998a,b,c; Masselink and Pattiaratchi, 2001a,b). Energetic wave conditions combined with equipment constraints have, until now, prevented a complete record of hydrodynamic measurements over the sea breeze cycle.

We hypothesized that beach profiles that were perched on rock structures would be better protected from waves and currents than profiles not fronted by rock. To test this, it was important to investigate: (1) temporal variations over the sea breeze cycle; and (2) spatial variations at different areas of the nearshore to identify how the rock structures influence the waves and currents. Therefore, there were four main objectives of the work, to:

- (i) Quantify temporal variations of waves and currents during the sea breeze cycle at locations:
 - a) offshore;
 - b) 20 m seaward of the limestone reef;
 - c) inside the lagoon; and
 - d) in the surf zone fronting the Exposed Profile and the Sheltered Profile.
- (ii) Quantify the response of the beach to the variation in currents and waves induced by the sea breeze cycle at an exposed beach profile and a sheltered beach profile.

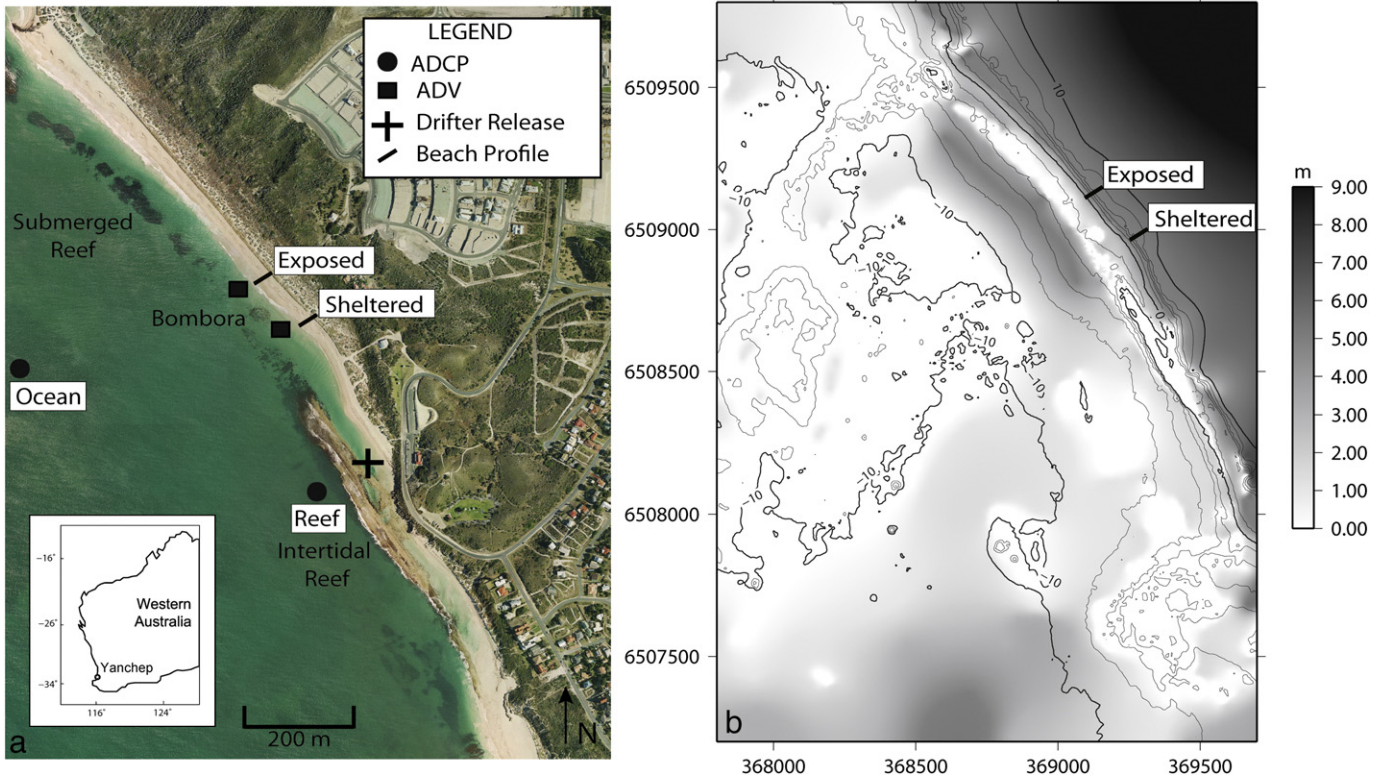


Fig. 2. Map showing (a) location of Yanchep Lagoon and aerial photo (source: Landgate) showing locations of instrument deployments; and (b) bathymetry contours of Yanchep Lagoon where the color bar indicates the estimated depth of sediment above the rock substrate in February 2010. White areas are where rocks outcrop above the sediment surface.

2. Study area

The coast of southwest Western Australia is characterized by a system of rocky shores and sandy beaches with significant compartmentalization. Yanchep is located in the Whitfords–Lancelin Sector in the classification by Searle and Semeniuk (1985) (Fig. 2a) which is characterized by unique marine ridge-and-depression morphology, limestone rocky shores and isolated accretionary cusps of Holocene sediment. This sector is fronted by a series of shore-parallel limestone ridges that area located up to 6.4 km offshore and form the basis of the coastal bathymetry and onshore geomorphology. Spearwood Ridge forms the framework of the mainland coast; Garden Island Ridge closes with the coast at Point Becher Point and Point Peron and gradually diverges with the shore to join Rottnest Island 20 km offshore. North of Rottnest Island the ridge is broken by the Perth Canyon while south of Rottnest Island, Five Fathom Bank Ridge lies 20 km offshore (Masselink and Pattiaratchi, 2001b). Older limestone ridges exist further landward and underlie the Holocene sediment that comprises the modern dune and beaches of the coast (Semeniuk and Johnson, 1982). The field site at Yanchep fits this framework in two ways; first as a Holocene beach set in a depression of the Spearwood Ridge, and second as a local analog for the broader structure of the coast.

Yanchep Lagoon is 60 km north of the City of Perth at the northern limit of the Perth metropolitan area (Fig. 2). The beach faces the southwest with an aspect of 230° and consists of well-sorted, medium sand that is comprised mostly of quartz and skeletal material with d_{50} of 0.4 mm (Semeniuk and Johnson, 1982; Murphy, 2011). The beach is perched on the Pleistocene Tamala Limestone Formation (Playford et al., 1975) which consists mainly of undulated, cross-bedded eolinite that developed during several dune-building episodes (Semeniuk and Johnson, 1982). Part of the beach is fronted by a continuous, intermittently-emerged limestone reef, and part by fully-submerged limestone formations, with the rest is not directly fronted

to seaward by rock (Fig. 2b). The lagoon that is enclosed by the intertidal limestone reef is open at the northern end, where water exits after overtopping the reef (Fig. 2). At the time of the field work in February 2010, the main areas of available sediment were to the southwest of the Lagoon and seaward of the reef near the shore with sediment depths above the rocky substrate reaching up to 6 m (Fig. 2b).

The coast of southwest Western Australia is microtidal, with a mean spring tidal range of 0.6 m (Pattiaratchi and Eliot, 2009; Department of Defence, 2011) and a low-moderate energy wave climate of mostly south-southwest swell (Lemm et al., 1999; Bosserelle et al., 2011). Background swell is generated in the Indian and Southern Oceans, and during summer H_s is 1–2 m, and mean wave period less than 8 s while in winter H_s is 1.5–2 m and wave period increases (Lemm et al., 1999). The coast is subject to ~30 storms per year, concentrated in July (Lemm et al., 1999) and the summer months are dominated by the south-southwest sea breeze that blows obliquely-onshore at Yanchep Lagoon. This sea breeze is formed by the interaction of the local temperature difference between land and sea and the synoptic weather patterns (Tapper and Hurry, 1993). A west coast trough develops as hot air from central Australia rises at the west coast. The position of this trough varies and affects the occurrence, intensity and direction of the sea breeze (Kepert and Smith, 1992). An onshore trough favors strong sea breezes with early onset and vice versa for an offshore trough (Masselink and Pattiaratchi, 2001a). The effects of the sea breeze have been compared to a medium-scale storm event (Masselink and Pattiaratchi, 1998a).

3. Methods

Field work focused on a 5 day period from 1 to 5 February 2010 in summer. The two beach profiles measured were 120 m apart. The Sheltered Profile was close to the northern end of the limestone reef and directly fronted to seaward by submerged limestone that was

2 m below the water surface (Fig. 2). The Exposed Profile was north of a limestone block referred to as the bombora (Fig. 2a) and was not directly fronted seaward by outcropping limestone. The beach profiles were measured every 2 hours from 1 February 2010 at 1300 h until 5 February 2010 at 0800 h and were surveyed to Australian Height Datum (AHD), which is approximately Mean Sea Level (MSL). Profiles were measured across the beachface above MSL.

Steel poles were hammered into the beach at 1 m intervals along each profile. The pole tips were surveyed and changes in the beach profiles were recorded as the variation in the height of the poles above the beach surface. Elevations of the pole tops were not observed to change during the survey. An exception was when poles were further hammered into the beachface to prevent them being washed away. At such time they were re-measured before and after, and the change in elevation was corrected in beach profile measurements. Error in profile measurements was estimated at ± 0.03 m. The volume of the beach profiles was calculated above AHD for a 1 m wide transect assuming uniform beach profile elevation 0.5 m either side of each transect.

Four measurement stations were deployed to measure waves and currents (Fig. 2a). Two Acoustic Doppler Current Profilers (ADCPs) were deployed:

- (i) offshore of the limestone reef in 10 m water depth (referred to as Ocean); and
- (ii) 20 m seaward of the limestone reef in 5 m water depth (referred to as Reef).

The ADCP's sampled in bursts measuring a 60 s ensemble at 2 Hz every 20 min. The storm surge was calculated from Reef data by low-pass filtering hourly-averaged sea levels. Due to a malfunction, sea levels were not available from the Ocean ADCP data. Acoustic Doppler Velocimeters (ADV's) sampled at 2 Hz and were deployed in the surf zone fronting each of the two beach profiles (Exposed and Sheltered Surf Zones). When battery power was low the sampling resolution was lowered. Currents were measured 20 cm above the sea bed and an ADV was deployed once in the Exposed Surf Zone and twice in the Sheltered Surf Zone. Cross-shore currents consisted of north-easterly onshore currents that headed 50° and south-westerly offshore currents that headed 230° . Longshore currents were north-westerly and headed 320° and south-easterly heading 140° .

Five drifters containing Global Positioning Systems (GPS) receivers developed by Johnson and Pattiaratchi (2004) were deployed to measure surface current patterns and velocities from inside the lagoon. The drifters contained a GPS receiver and a logger which recorded the drifter latitude and longitude every 10 s to derive surface current tracks and velocity. These drifters have been shown to have only slight wind-drag effects and to be a suitable proxy for surface current speeds (Johnson and Pattiaratchi, 2004). The drifters were deployed from the southern end of the lagoon (Fig. 2a) four times, in the afternoon and in the morning: twice on 2 February and twice on 4 February (Table 2).

Wind data used in this study was obtained from the Australian Bureau of Meteorology and is from the nearest coastal weather station at Ocean Reef 25 km south of Yanchep, where measurements were taken 10 m above ground. Tidal variation during the study was diurnal with amplitude of 0.3 m, therefore tidal currents were negligible. Despite the low range, the magnitude of tides and storm surge can still influence on the hydrodynamics and sea-level measurements and are presented.

Autospectral analysis was undertaken on sea level and current components to calculate wave spectra on sections of 512 measurements. This was only possible while battery power was sufficient for high resolution sampling. Fast Fourier Transform was used to calculate a wave power spectrum which was high-pass filtered to remove infragravity waves, then smoothed using a Hanning window and detrended.

Wave refraction was calculated using a coupled wave model based on XBeach (Roelvink et al., 2009). The model solves the wave action balance equation, taking into account energy dissipation due to wave breaking and bottom friction and also wave-current interactions. The model is coupled to a roller model to account for the momentum transfer from wave breaking and currents and a current model. It is capable of reproducing the complex hydrodynamic circulation around the reef and lagoon, however only wave refraction patterns near the limestone reef are presented here.

4. Results

4.1. Wind speeds and directions

Wind speeds at Ocean Reef clearly showed the onset of the sea breeze by a rapid increase in velocity and change in direction from east ($100\text{--}150^\circ$) to south-southwest (200°) (Fig. 3b) which is onshore at Yanchep Lagoon. On 1–3 February sea breeze onset was at 0930 h, while on 4 February 2010 was at 1230 h. On each day, the wind speeds before the onset of the sea breeze were $3\text{--}10\text{ m s}^{-1}$ (Fig. 3a) increasing until 2000 h and reached daily maxima of $12\text{--}17\text{ m s}^{-1}$ on 1–4 February. Peak wind speeds were: 12 m s^{-1} on 1 February, 17 m s^{-1} on 2 February, 14 m s^{-1} on 3 February, 12 m s^{-1} on 4 February and 8 m s^{-1} on 5 February.

4.2. Ocean and reef current changes during sea breeze

Changes in the depth-averaged longshore and cross-shore currents measured after the onset of the sea breeze at the two ADCPs, are summarized in Table 1. On 1 February, depth-averaged longshore currents were similar ($\sim 0.02\text{ m s}^{-1}$) at the Reef and Ocean sites, and in the afternoon during the sea breeze increased to 0.05 m s^{-1} and 0.03 m s^{-1} respectively (Fig. 3e and Table 1). Cross-shore currents increased from almost nil in the morning, to strongly offshore in the afternoon with a maximum speed of -0.05 m s^{-1} at the Ocean site and 0.03 m s^{-1} at the Reef (Fig. 3h and Table 1).

Early on 2 February, longshore currents at the Reef and Ocean sites were north-westerly at $\sim 0.04\text{ m s}^{-1}$ (Fig. 3e). In the late morning there was a rapid decrease in current speed at the Ocean site to almost zero (Table 1). From the early afternoon to late evening, longshore currents at both locations increased with the onset of the sea breeze. Reef currents doubled from 0.05 to 0.1 m s^{-1} and Ocean currents increased from zero in the late morning to 0.08 m s^{-1} in the late evening. Cross-shore currents were offshore and increased in a similar manner from -0.04 m s^{-1} at both locations in the early morning to reach -0.1 m s^{-1} at the Reef and Ocean sites in the late evening (Fig. 3h and Table 1).

On 3 February longshore currents at the Reef and Ocean sites were both north-westerly with Reef currents generally higher (0.03 m s^{-1}) than Ocean currents (0.02 m s^{-1}) (Fig. 3e and Table 1). Cross-shore currents decreased in the early hours of the morning then increased in the afternoon with the onset of the sea breeze with Reef currents just -0.07 m s^{-1} compared to more than -0.1 m s^{-1} for Ocean currents (Fig. 3h and Table 1).

On 4 February longshore currents at both sites decreased in the morning to almost zero in the early afternoon, then from early afternoon Reef currents rapidly increased to more than 0.05 m s^{-1} with no such increase in Ocean currents (Fig. 3e). Cross-shore currents at the Ocean site increased slightly in speed throughout the day, with Reef currents flowing onshore in the late morning, then rapidly offshore and increasing in speed at the onset of the sea breeze (Fig. 3h).

On 5 February, longshore currents at the Ocean site were north-westerly, less so for Reef currents (Fig. 3e and Table 1). Reef and Ocean cross-shore currents were considerably different. For most of the day Reef currents were onshore whereas Ocean currents were offshore (Fig. 3h and Table 1).

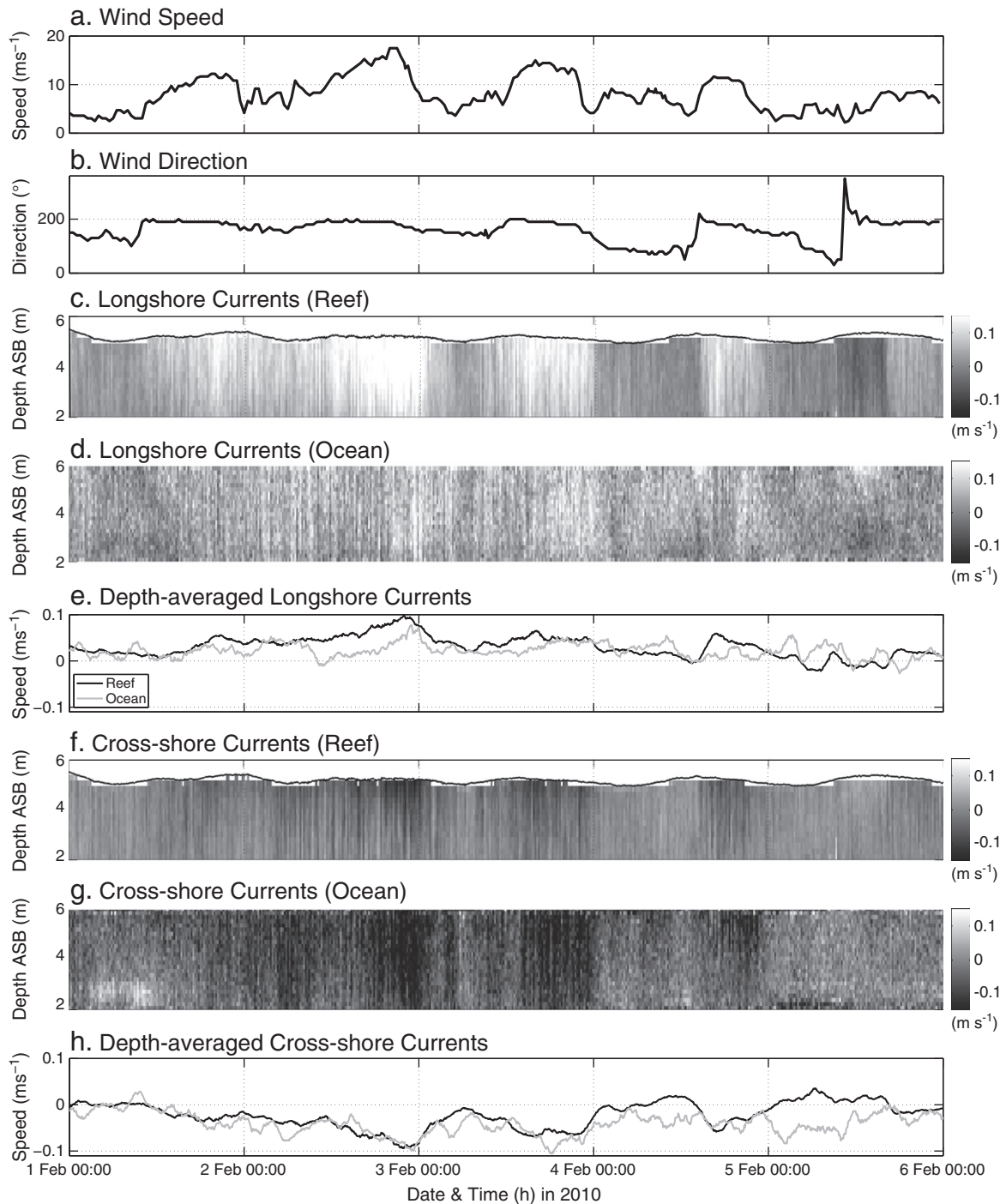


Fig. 3. (a) and (b) show wind speed and direction at Ocean Reef, (c) and (d) show the longshore currents at the Reef and Ocean sites where positive is NW, (e) shows the depth-averaged longshore currents, (f) and (g) show the cross-shore currents at the Reef and Ocean sites where positive is onshore, and (h) the depth-averaged cross-shore currents. Lines indicate onset of the sea breeze on each day.

4.3. Lagoonal current patterns

Currents from inside the lagoon were measured using five GPS drifters in four deployments, with results summarized in Table 2 and drifter paths shown in Fig. 4. During drifter deployment 1 in the early afternoon on 2 February when wind speed was 12 m s^{-1} , all drifters traveled only to the end of the lagoon where they were washed onshore by wave action. Mean and maximum surface currents were 0.61 and 1.06 m s^{-1} (Table 2).

During drifter deployment 2 on 2 February in the late afternoon when wind speed was 15 m s^{-1} , there was a large difference to results

from the previous deployment. Three of the drifters washed onshore at the end of the lagoon while two traveled further north of the lagoon and one not coming onshore until at the bombora (Fig. 4). There was evidence of a clockwise current south of the bombora. Mean and maximum surface currents were 0.65 and 1.65 m s^{-1} . Surface currents inside the lagoon during drifter deployment 2 were $0.3\text{--}0.8 \text{ m s}^{-1}$ and exiting were up to 1 m s^{-1} where mean longshore surface currents in the lagoon exit measured with an ADCP were 0.4 m s^{-1} .

During drifter deployment 3 in the morning on 3 February, the drifters traveled the furthest of any of the deployments when wind speed was 8 m s^{-1} . Two were washed onshore between the lagoon

Table 1
Summary of depth-averaged current changes after the onset of the sea breeze at the Reef and Ocean sites.

Before/after sea breeze onset	1 Feb	2 Feb	3 Feb	4 Feb	5 Feb
Reef (ms^{-1})					
Longshore	0.02/0.05	0.05/0.1	0.03/0.5	0.03/0.02	0.02/0.02
Cross-shore	0/−0.03	−0.04/−0.1	−0.03/−0.07	0.01/−0.05	0.02/−0.02
Ocean (ms^{-1})					
Longshore	0.02/0.03	0/0.08	0.02/0.04	0.02/0.04	0.03/0.02
Cross-shore	0/−0.05	−0.04/−0.1	0.03/−0.1	−0.05/0.05	−0.05/−0.03

entrance and the bombora whilst three traveled around the bombora in a clockwise eddy. Current speeds were slow compared to the afternoon deployments on the previous day. Mean and maximum surface current speeds were 0.24 and 1.03 m s^{-1} . A halving of the wind speed between drifter deployments 2 and 3 effectively halved the surface current speeds in the lagoon.

In the afternoon of 3 February during drifter deployment 4 wind speed was 14 m s^{-1} and the drifters only traveled to the end of the lagoon before being washed to shore by wave action, like occurred in the early afternoon on the previous day. Mean and maximum surface current speeds were 0.25 and 0.70 m s^{-1} .

Wave ray-tracing obtained from XBeach (Roelvink et al., 2009) represented the mean direction of wave propagation (Fig. 5). It indicated how waves refract around the limestone reefs, in particular around the lagoon exit. Converging ray traces show wave energy focused on the Bombora north of the lagoon. After the onset of the sea breeze, waves were more southerly (Fig. 5a) than before the onset when swell dominated (Fig. 5b). Despite this difference in offshore wave direction, the reefs forced the direction of the swell and sea breeze waves to be similar in the nearshore. This led to similar wave driven current patterns as observed with the drifters (Fig. 4).

4.4. Surf zone waves and currents

Waves and bottom-currents 20 cm above the sea bed were measured in the surf zone fronting the two beach profiles. On 1 February, longshore currents at the Exposed and Sheltered Surf Zones had similar speeds at less than 0.1 m s^{-1} . From 1800 h currents at the Sheltered Surf Zone became onshore and stronger reaching 0.3 m s^{-1} and Exposed Surf Zone currents did not change (Fig. 6a). From 0000 h on 2 February, currents at both surf zone locations were onshore, with stronger currents at the Exposed Surf Zone. Longshore current speeds increased in the afternoon on 1 February, when high swell and strong winds developed and currents at the Exposed Surf Zone were consistently stronger than at the Sheltered Surf Zone. On 4–5 February, currents at the Sheltered Surf Zone were near zero (Fig. 6b).

Table 2
Summary of drifter deployments where Dep. No. is deployment number and wind is direction (from) measured at Ocean Reef.

Dep. No.	Date and Time in 2010	Wind Speed and Direction	Pattern	Mean current speed	Maximum current speed
1	2 Feb 1250–1300 h	12 m s^{-1} S	All onshore at lagoon exit	0.61 m s^{-1}	1.06 m s^{-1}
2	2 Feb 1650–1700 h	15 m s^{-1} S	3 onshore at lagoon exit, 2 eddy clockwise near bombora	0.65 m s^{-1}	1.65 m s^{-1}
3	3 Feb 0850–0930 h	8 m s^{-1} SE	All reached near to bombora in clockwise eddies	0.24 m s^{-1}	1.03 m s^{-1}
4	3 Feb 1520–1550 h	14 m s^{-1} S	All onshore at lagoon exit	0.25 m s^{-1}	0.70 m s^{-1}

In the afternoon on 1 February cross-shore currents at the Exposed and Sheltered Surf Zones were slow at less than 0.1 m s^{-1} and onshore in the Sheltered Surf Zone and offshore in the Exposed Surf Zone (Fig. 6c). On 2 February at 0000 h cross-shore currents in the Sheltered Surf Zone were 0.5 m s^{-1} , then decreased to become offshore later in the morning. Pressure, pitch and heading data showed that the instrument was not moving at this time although it may have been obstructed by drifting wrack to cause such a rapid change in current speed and direction. During this period of rapid change on 1 February, currents at the Exposed Surf Zone were offshore and stable at $\sim 0.25 \text{ m s}^{-1}$. On the second half of 1 February until the morning of 2 February when measurements stopped, currents in the Sheltered Surf Zone had stabilized and headed onshore at $\sim 0.2 \text{ m s}^{-1}$ while the currents in the Exposed Surf Zone were mostly offshore at 0.4 m s^{-1} . The second deployment at the Sheltered Surf Zone shows stable and slow cross-shore currents (Fig. 6d).

Sea level was lowest during Deployment 1 on 1 February at 1400, a daily maximum at 2200 h, then on 2 February a daily minimum at 0600 h (Fig. 6e). A daily maximum occurred during Deployment 2 at 1400 h on 4 February and a minimum at 0400 on 5 February (Fig. 6f). On 1 February from the late morning swell and wind wave heights were both 0.3 – 0.4 m , with slightly higher wind waves in the afternoon (Fig. 6k). Swell wave height increased from 0500 h on 2 February and reached a daily maximum of $\sim 0.8 \text{ m}$ in the early afternoon. There was also a slight increase in wind wave height from mid-morning with a maximum of 0.5 m in the early afternoon (Fig. 6k). From then there was no wave data due to low batteries and insufficient sampling rates, until 4 February when swell and wind waves had similar heights of 0.2 – 0.4 m (Fig. 6l). Mean wave period was similar at both sites during deployment 1 at 5 s on 1 February, and increased on 2 February from mid morning with a high period at the Sheltered Surf Zone of up to 8 s , with only a slight increase at the Exposed Surf Zone of up to 5 s (Fig. 6i). During deployment 1 H_s was $\sim 0.2 \text{ m}$ and increased at the Sheltered Surf Zone to 0.5 – 0.6 m compared to less than 0.5 m at the Exposed Profile from the late morning (Fig. 6g). Overnight, H_s at both sites was $\sim 0.6 \text{ m}$ then at the onset of the sea breeze on 2 February increased to more than 1 m at the Sheltered Surf Zone while the daily maximum at the Exposed Surf Zone was 0.8 m .

4.5. Beachface profile changes

4.5.1. Two-hourly beach volume changes during sea breeze

The erosional and accretional responses of beachface morphology to the sea breeze cycle are clearly visible in Fig. 7. The tidal range was just 30 cm over the period of the field survey, with storm surge only a minor component of the sea level. From 1 February, the storm surge decreased with the onset of a high-pressure system. Sea level reached a minimum in the late morning of 4 February after a decrease of 13 cm and it then began to increase again (Fig. 7a).

There were larger changes in sediment volume at the Sheltered Profile that was immediately landward of submerged reef (Fig. 7c) compared to the Exposed Profile (Fig. 7b). Until 3 February both profiles had the same pattern of erosion and accretion albeit with different volume changes. Both profiles eroded on 2 February although the Sheltered Profile had double (7 m^3) the volume of erosion of

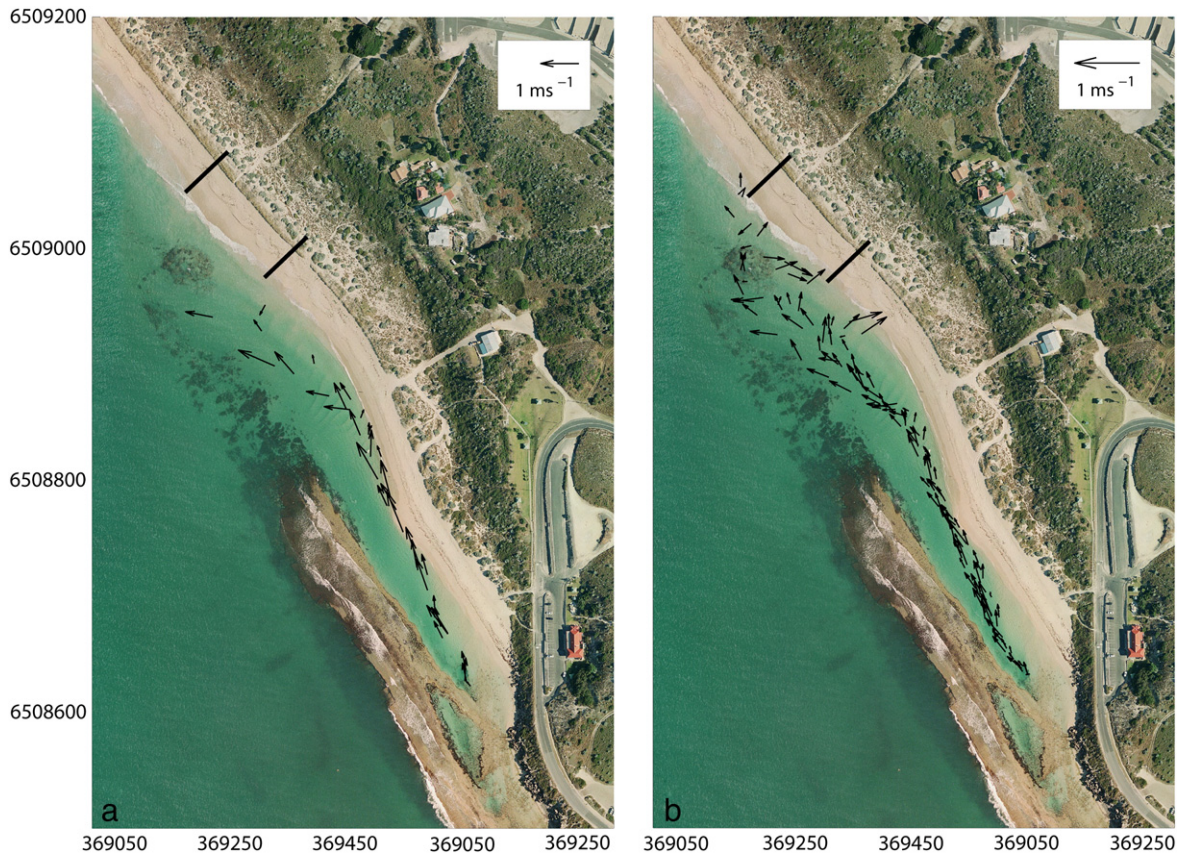


Fig. 4. Drifter velocity vectors from (a) Feb 2 at 1640–1700 h; and (b) Feb 3 2010 at 0840–0930, where black lines show the two beach profiles measured (modified from Gallop et al., 2011).

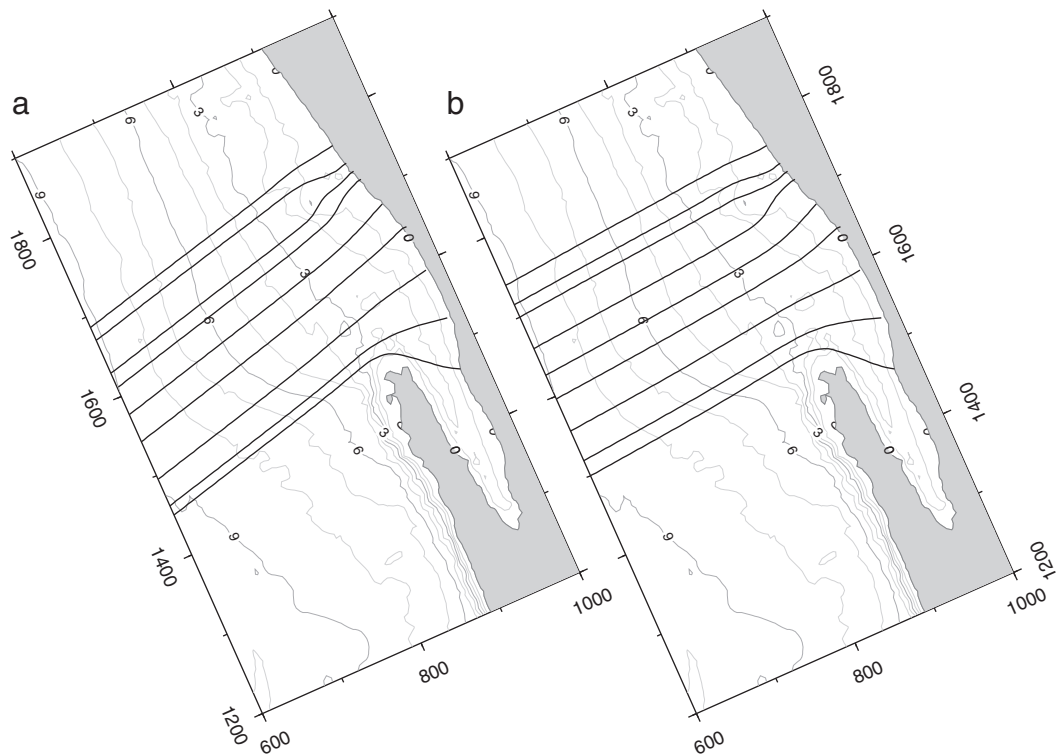


Fig. 5. Model snapshot of wave ray trace using XBeach showing wave refraction and current direction around end of Yanchep reef—(a) during a sea breeze event and (b) during a swell event.

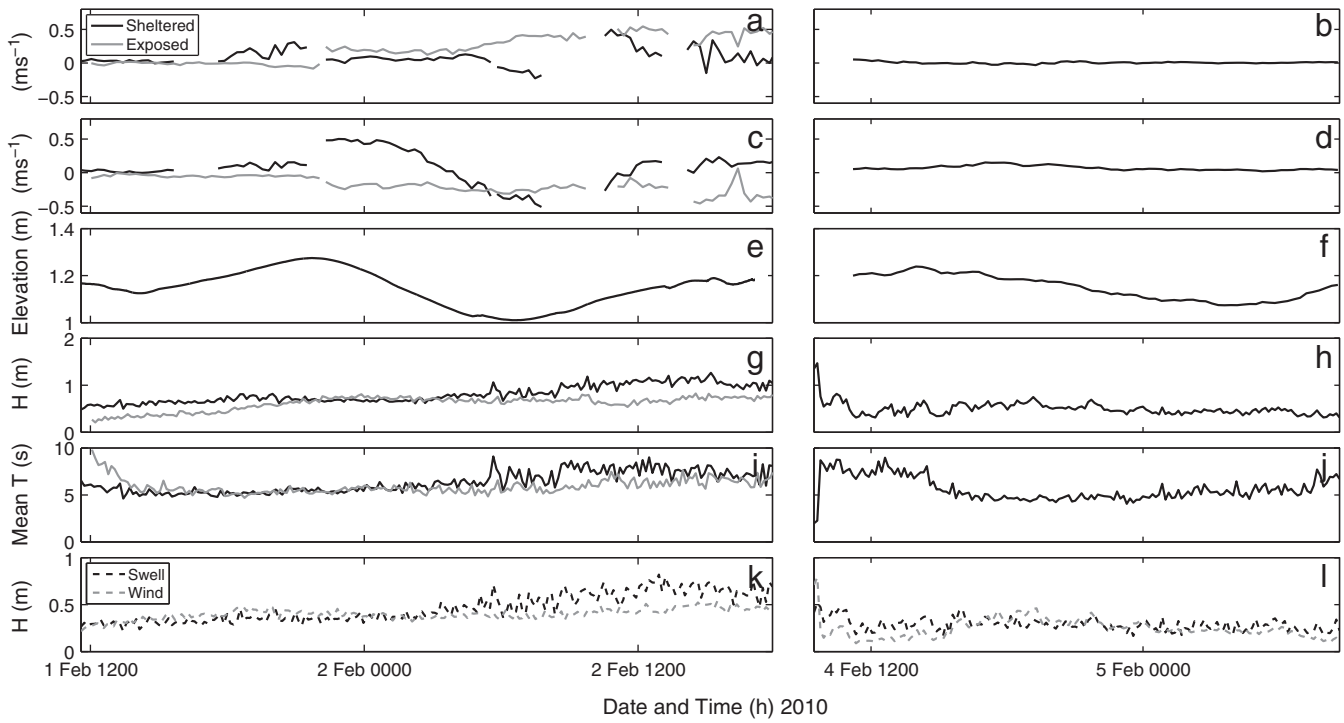


Fig. 6. Bottom currents and waves from deployments 1 and 2 for the Exposed and Sheltered Surf Zones. (a and b) show mean longshore currents (positive NW); (c and d) mean cross-shore currents (positive onshore); (e and f) show sea level in the Sheltered Surf Zone; (g and h) significant wave height; (i and j) mean wave period; and (k and l) mean wave height of swell and sea in the Sheltered Surf Zone.

that occurred at the Exposed Profile in 2 h. On 2 February both profiles accreted then eroded from midday, with the Sheltered Profile accreting at a faster rate with a daily maximum of 0.8 m^3 at the

Sheltered Profile compared to maximum of 0.5 m^3 at the Exposed Profile. Similarly, after midday on 2 February the Sheltered Profile eroded at a faster rate of up to 1.7 m^3 in 2 h compared to up to

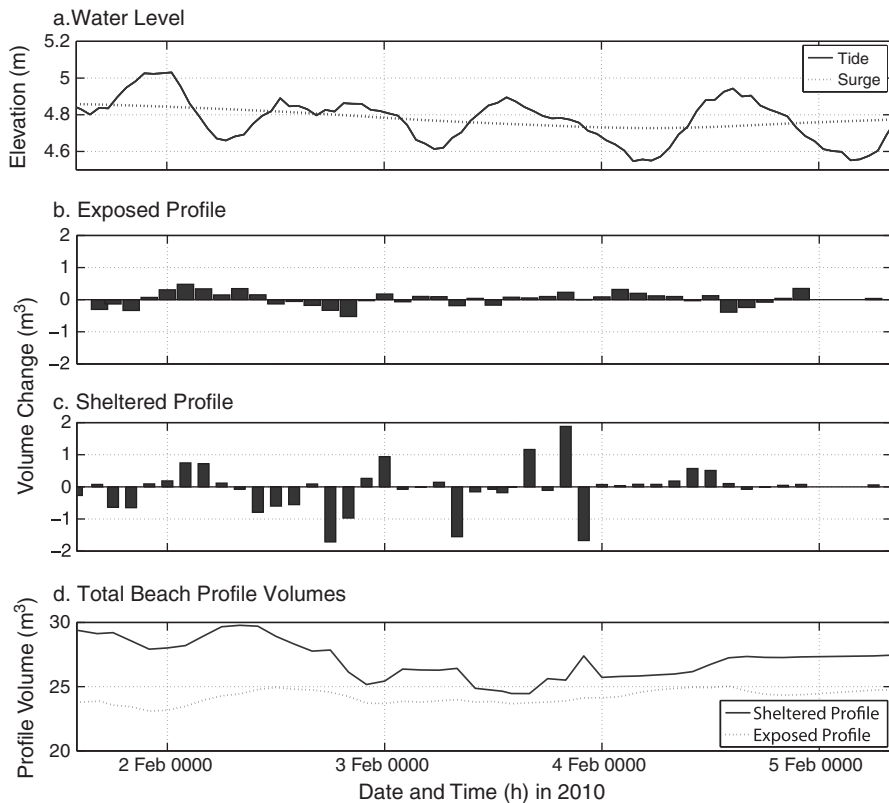


Fig. 7. (a) shows the tide and storm surge at the Reef, (b) and (c) changes in beach profile volumes above AHD between measurements for Exposed and Sheltered Profiles and (d) shows total profile volume above AHD for the Exposed and Sheltered Profiles.

0.5 m³ in 2 h for the Exposed Profile. On 3 February the patterns of profile behaviour differed more, with smaller rates of volume change at the Exposed Profile compared to the Sheltered Profile. From 2 February at 0000 h the Exposed Profile accreted at a low rate of <0.03 m³/h with minor erosion in the afternoon on 4 February. At the Sheltered Profile, from 3 February at 0000 h the profile generally eroded in the morning, with some accretion in the afternoon and evening and low rates of accretion on 4 February.

The volume of sediment eroded from the Sheltered Profile on 1 February was 6 m³ more than that of the Exposed Profile. However, during 2 February with high swell and strong winds the Sheltered Profile eroded more than the Exposed Profile (Fig. 7d). On 1 and 2 February a cycle in beach volume analogous to the sea breeze cycle is clearly visible. On the second half 1 February the beach volume at both profiles decreased, and after 2 February at 0000 h the beach volume increased. The profiles accreted when the wind speed decreased, then eroded during the second half of the day. On 3 February the Exposed Profile was remarkably stable and there was a little erosion and accretion at the Sheltered Profile. On 4 February the Sheltered Profile volume increased in the afternoon while the Exposed Profile decreased.

4.5.2. Backshore vs. foreshore beach profile change

Changes in the beach profile elevation at two different levels on the beachface were calculated. The two different levels of the beachface were defined according to typical beach profile terminology (Komar, 1998): (1) from the dune toe to the berm—the backshore; and (2) below the berm down to sea level—the foreshore (Fig. 8a). The position of the berm on the beachface was relatively stable, changing by only up to 20 cm vertically. The berm at the Exposed Profile varied between 1.4 and 1.6 m above AHD (Fig. 8a–d), and at the Sheltered Profile between 1.8 and 1.9 m above AHD (Fig. 8e–h). Profiles were compared between 1000 h and 1800 h daily, except on 1 February when profiles were not measured until the afternoon and the earliest measurement was taken at 1400 h.

During the sea breezes on 1–3 February the foreshore of both beach profiles eroded, generally with slight accretion on the backshore of the Exposed but not at the Sheltered Profile except on 2 February (Fig. 8). On 4 February, the two beach profiles behaved differently with the foreshore at the Exposed Profile eroding and the backshore accreting

(Fig. 8d). The foreshore of the Sheltered Profile accreted with only a small amount of accretion in the backshore (Fig. 8h).

Two-hourly changes in the mean elevation of the backshore and foreshore at the two beach profiles shows that overnight on 1 February, the backshore and foreshore at the Exposed Profile both eroded while at the Sheltered Profile there was evidence of some overnight accretion along the profile (Fig. 9). During the sea breeze on 2 February, the backshore of both profiles accreted in the morning, with mostly erosion of the foreshore in the afternoon, and some accretion of the backshore. Overnight, the Exposed Profile mostly eroded, compared to accretion of the Sheltered Profile. On 3 February, both profiles had similar behavior during the sea breeze compared to 4 February when the Exposed Profile changed from accretion in the foreshore, to erosion of the foreshore and accretion of the backshore. While at the Sheltered Profile, there was accretion of the foreshore and slight accretion of the backshore. Overall, the backshore of the Exposed Profile appeared to accrete more than the Sheltered Profile. Only a fraction of the sediment eroded from the foreshore was deposited on the backshore.

4.5.3. Total beach volume during sea breeze and recovery

Overall, during the sea breeze on 1 February, the Exposed and Sheltered Profiles both eroded by 0.19 m³ per m of beach width (Fig. 10b). Overnight on 1 February both beach profiles recovered by accreting by 0.87 m³ at the Exposed Profile and 0.58 m³ at the Sheltered Profile (Fig. 10c). Profile on 2 February the Sheltered Profile eroded by nine times more than the Exposed Profile, at 1.85 m³ compared to just 0.21 m³ at the Exposed Profile (Fig. 10b). Overnight there was no beach profile recovery, both profiles eroded, by 0.58 m³ at the Exposed and 1.43 m³ at the Sheltered (Fig. 10c). On 3 February the Exposed Profile did not change during the sea breeze but the Sheltered Profile accreted by 0.75 m³ (Fig. 10b). More substantial recovery occurred on the Exposed Profile where it accreted by 1.06 m³ compared to 0.37 m³ on the Sheltered Profile (Fig. 10c). On 4 February the Exposed Profile eroded by a total volume of 0.54 m³ while the Sheltered Profile accreted by 1.11 m³ (Fig. 10b). Overnight there was slight recovery at both profiles, when the Exposed Profile accreted by 0.35 m³ compared to 0.18 m³ at the Sheltered (Fig. 10c).

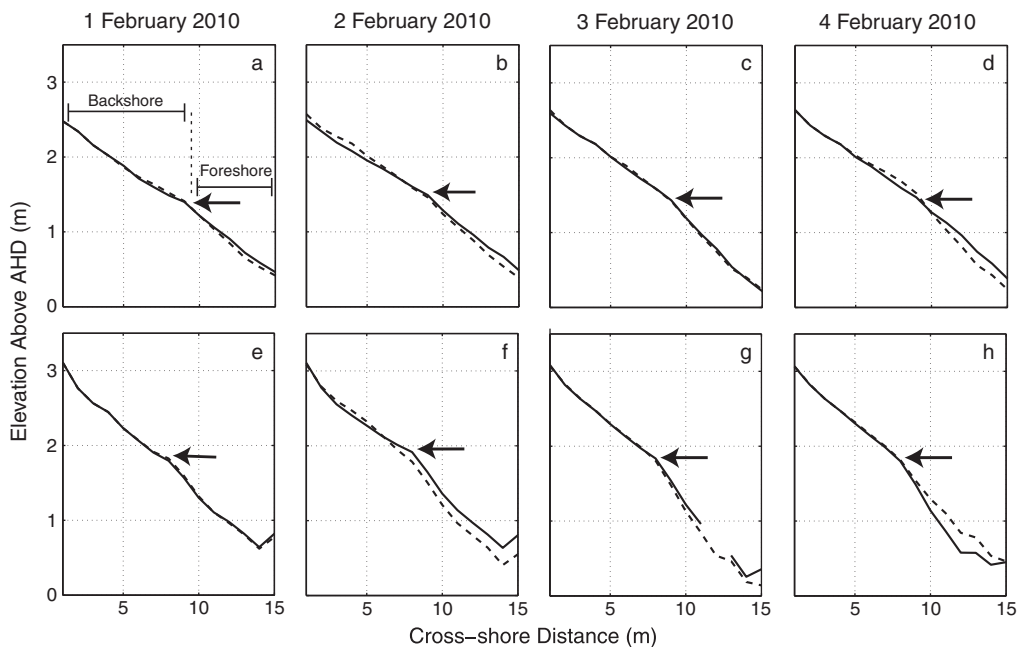


Fig. 8. Beachface profiles before and after onset of sea breeze, where (a)–(d) show the Exposed Profile and (e)–(h) the Sheltered Profile. Solid line indicates pre-sea breeze (1000 h except on 1 February at 1400 h) and dashed line post-sea breeze at 1800 h. The berm is indicated by the arrow, and definition of the backshore and foreshore shown in (a).

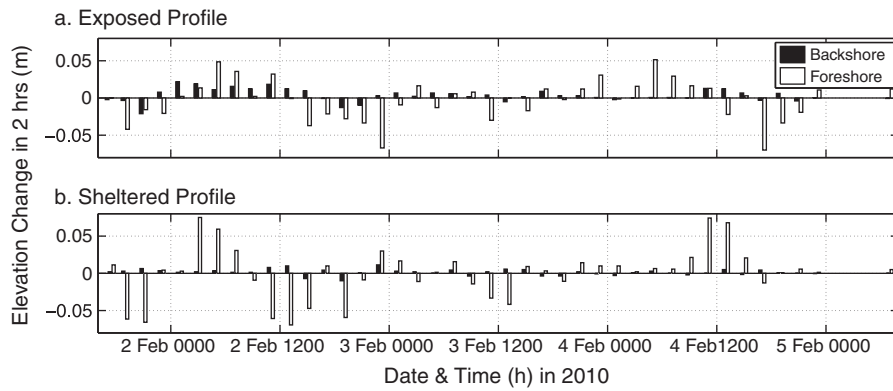


Fig. 9. Mean change in profile elevation every 2 h at (a) the Exposed Profile and (b) the Sheltered Profile, in the backshore and foreshore.

5. Discussion

Our original hypothesis that perched beaches are often more stable than non-perched beaches (Larson and Kraus, 2000; Vousdoukas et al., 2007) was not supported by our results. The perched, Sheltered Profile had greater changes in sediment volume during the sea breeze cycle compared to the non-perched, Exposed Profile (Figs. 7–10). This was likely due to the strong current jet exiting the lagoon near the Sheltered Profile and likely will not be the case for all types of natural perched beaches. The beach profile behavior on 3 and 4 of February was different to 1 and 2. On 1 and 2 February, both beach profiles eroded during the sea breeze. Conversely, on 3 February the Exposed Profile was stable overall and on 4 February it eroded while on both days the Sheltered Profile accreted (Fig. 8). Weaker lagoonal currents (Table 2) due to weaker sea breezes on 3 and 4 of February were likely responsible for the accretion of the Sheltered Profile because incoming waves could wash this sediment onshore rather than it being directed offshore by the current jet.

There was a large degree of spatial variation in the waves and currents around the limestone structures. The current inside the lagoon was extremely sensitive to changes in magnitudes of wave-overtopping of the limestone reef during the cycle of the sea breeze, which forced the longshore current. Despite being located just 120 m apart and having similar pre-sea breeze magnitudes and

directions, bottom currents in the Exposed and Sheltered Surf Zones differed in their response to the sea breeze activity. Cross-shore currents in the Sheltered Surf Zone tended to be stronger and more onshore compared to currents in the Exposed Surf Zone which tended to be slower but offshore, similar to findings of Pattiaratchi et al. (1997) at a non-perched sandy beach in southwest Western Australia. Currents in the Sheltered Surf Zone were in an area of high geological influence and were more affected by the jet exiting the lagoon which forced the current shoreward and thus overturned the expected cross-shore currents generated by the surf. Longshore currents during the sea breeze were sometimes stronger in the Sheltered Surf Zone such as 1 February. However, on 2 February currents were stronger in the Exposed Surf Zone and headed south-easterly for a few hours after the onset of the sea breeze rather than the usual north-westerly in the direction of the sea breeze. This shift in direction was likely due to wave breaking on the bombora that locally increased the sea level to create currents that flowed to the north and south. These currents were captured during drifter deployments 2 and 3 and wave energy focusing and breaking on the bombora was revealed by way ray tracing using XBeach (Fig. 5). This energy focusing caused set-up on the bombora and the lee side (Fig. 5) and water was discharged through troughs to the north and the south that created a clockwise eddy on the south side of the bombora, similar to the

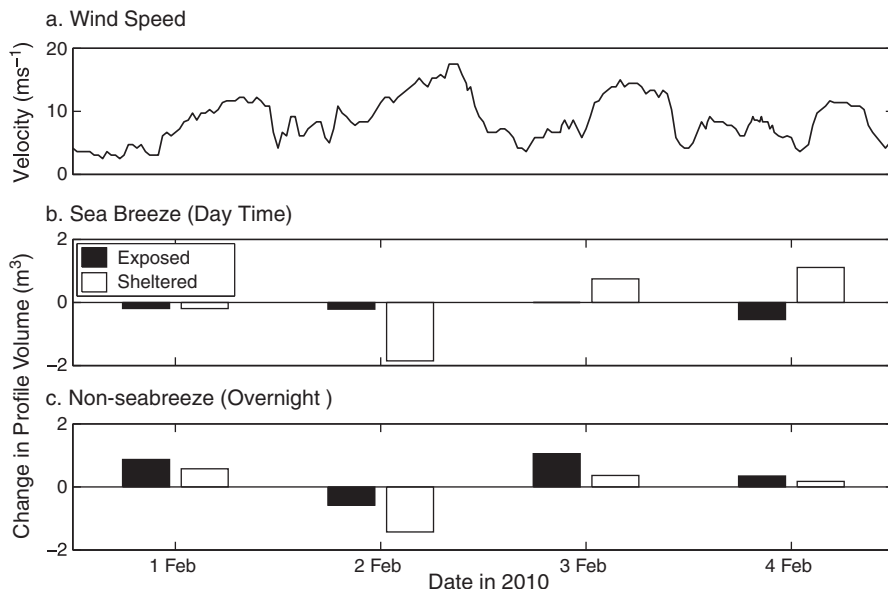


Fig. 10. (a) shows wind speed at Ocean Reef and (b) total beach profile volume change per unit m of beach width during sea breeze where 1 February was between 1400 h and 1800 h and other days between 1000 h and 1800 h and (c) total beach profile volume change overnight between 1800 and 0800 the following day.

circulation model described by Ranasinghe et al. (2006) around an artificial surfing reef. Currents at the Exposed Surf Zone were not affected by this current pattern while Sheltered Surf Zone currents were.

Overnight when wind speeds decreased, both profiles accreted, and the Exposed Profile recovered by 1.5–5 times more, consistent with work by Muñoz-Pérez and Medina (2010). It has been suggested that rocky outcrops impede onshore sediment transport due to a scour step at the seaward margin (Turner, 2000; Vousdoukas et al., 2009). Due to sustained winds and swell waves, on 2 February both profiles continued eroding overnight and the Sheltered Profile lost 2.5 times more volume than the Exposed Profile (Fig. 10c). Greater changes in volume at the Sheltered Profile suggest that the lagoon current (Fig. 4) was driving this magnified response, and perhaps inhibiting overnight accretion. This observation is supported by: (1) strong cross-shore currents in the Sheltered Surf Zone (Fig. 6c) compared to a stronger longshore component in the Exposed Surf Zone (Fig. 6a); and (2) wave energy focusing on the bombora and wave refraction patterns found by wave ray tracing and drifter tracks (Figs. 4 and 5).

The greater volumes of erosion at the Sheltered compared to the Exposed Profile on 2 February is in agreement with Vousdoukas et al. (2007). They found that although relict (submerged) beachrock may provide some coastal protection by reducing wave energy reaching the shore, modern (emerged) beachrock may in fact promote offshore loss of unconsolidated beach sediments. Similarly, Dean et al. (1997) found that an offshore breakwater increased the erosion rate above the background level by ~130%. These findings are opposite to what was suggested from a numerical modeling study by Larson and Kraus (2000) who assumed that a hard-bottom will impose a strain on the sand transport rate, and that it will restrict sand movement because the area it occupies does not contribute to the sediment budget. Larson and Kraus (2000) did however focus only on cross-shore sand transport, assuming that longshore sand transport was zero or uniform. The longshore transport of sediment at Yanchep Lagoon is a significant component of the perched beach dynamics, due to the obliquely-onshore direction of the sea breeze as well as the presence of the current jet exiting the lagoon in a longshore direction.

Further field investigations at different sites, under different geologic frameworks and at different time scales are required to develop a detailed understanding of perched beach behavior. Beach groundwater is also likely to influence sediment transport on perched beaches. In this work, due to logistical constraints beach profile measurements were not taken below MSL, but would be valuable to show where sediment eroded from the beachface is deposited. While measured intensively and selected for their contrasting locations, just two beach profiles were used. As indicated in Fig. 1, the geomorphic forms of perched beaches are extremely variable and even at the short stretch of shore at Yanchep Lagoon the geology varies significantly. Research is currently under way at Yanchep Lagoon to investigate the beach response during a storm, and at longer time scales including seasonal and decadal. However, this present study is regarded as a first step in understanding coastal processes and morphological responses on a beach type that has attracted little research attention to date despite its common occurrence around the Australian coast and the globe.

6. Conclusions

This work shows that beaches that are perched on rock structures may not be better protected from waves and currents than exposed profiles. The Sheltered Profile that was fronted seaward by submerged limestone that was 2 m deep had greater volume changes than the Exposed Profile that was not fronted directly seaward by limestone. However, the Exposed Profile recovered more by overnight accretion. This indicates that perched beaches may not be better protected than non-perched beaches, contrary to the general consensus. There was a strong degree of spatial variation in waves and

currents around the limestone structures. For example, compared to Ocean and Reef currents, the lagoonal current response to the sea breeze activity was substantially magnified due to changes in wave overtopping of the reef which drove the flow. Surf zone currents near the end of the lagoon were forced shoreward by the lagoon jet. Wave refraction patterns around the reef were revealed with GPS drifter tracks and wave-ray tracing using XBeach and had similar patterns during sea breeze and swell-wave dominated events. This work lays a foundation for more research on perched beach hydrodynamics and morphodynamics, and has relevance for much of the WA coast, the rest of Australia and other coasts world-wide.

Acknowledgements

This work was undertaken by S.L.G as part of a PhD at The University of Western Australia and was funded by the Samaha Research Scholarship and the Western Australian Marine Science Institution (WAMSI, project 6.1). Thank you to the Australian Bureau of Meteorology for supplying wind data and to the Department of Transport for supplying Rottneest Island wave data and for undertaking some of the surveying, specifically to Karl Ilich and Lucia Roncevic for organizing the work. We are extremely grateful to field helpers: Dennis Stanley, Didi, Amandine Bosserelle, Nicky Gallop, Saif Ullah-Farooqi, Ivan Haigh, Asha de Vos, and the Yanchep Surf Life Saving Club. Finally thank you to Michael Collins for his suggestions regarding this work, to Carey Conn for editing the manuscript and to comments from the Editor, J. J. Muñoz-Pérez and an anonymous reviewer.

References

- Bartrum, J.A., 1926. "Abnormal" shore platforms. *The Journal of Geology* 34 (8), 793–806.
- Bosserelle, C., Pattiaratchi, C., Haigh, I.D., 2011. Inter-annual variability and longer-term changes in the wave climate of Western Australia between 1970 and 2009. *Ocean Dynamics*. doi:10.1007/s10236-011-0487-3.
- Chowdhury, S.Q., Falzul, A.T.M., Hasan, H.K., 1997. Beachrock in St. Martins Island, Bangladesh: implications of sea level changes on beachrock cementation. *Marine Geodesy* 20 (1), 89–104.
- Cleary, W.J., Riggs, S.R., Marcy, D.C., Snyder, S.W., 1996. The influence of inherited geological framework upon a hardbottom-dominated shoreface on a high-energy shelf, Onslow Bay, North Carolina, USA. Special Publication, 117. Geological Society, London, pp. 249–266.
- Da Silva, C., 2010. A perched beach typology of the Ningaloo, Perth and Esperance coasts, Western Australia, MSc Thesis, School of Earth and Environment, The University of Western Australia, Crawley, Western Australia, Australia.
- Dean, R.G., Chen, R., Browder, A.E., 1997. Full scale monitoring of a submerged breakwater, Palm Beach, Florida, USA. *Coastal Engineering* 29, 291–315. doi:10.1016/S0378-3839(96)00028-2.
- Department of Defence, 2011. Australian National Tide Tables 2011. Australian Hydrographic Publication, Canberra.
- Dickinson, W.R., 1999. Holocene sea-level record on Funafuti and potential impact of global warming on central Pacific Atolls. *Quaternary Research* 51, 124–132. doi:10.1006/qres.1998.2029.
- Doucette, J.S., 2009. Photographic monitoring of erosion and accretion events on a platform beach, Cottosloe, Western Australia, paper presented at 33rd International Association of Hydraulic Engineering and Research Biennial Congress. IAHR, Vancouver, Canada.
- Eversole, D., Fletcher, C.H., 2003. Longshore sediment transport rates on a reef-fronted beach: field data and empirical models Kaanapali Beach, Hawaii. *Journal of Coastal Research* 19 (3), 649–663.
- Fitzgerald, D.M., van Heteren, S., Montello, T., 1994. Shoreline processes and damage resulting from the Halloween Eve Storm of 1991 along the north and south shores of Massachusetts Bay, U.S.A. *Journal of Coastal Research* 10 (1), 113–132.
- Frihi, O.E., El Ganaini, M.A., El Sayed, W.R., Iskander, M.M., 2004. The role of fringing coral reef in beach protection of Hurghada, Gulf of Suez, Red Sea of Egypt. *Ecological Engineering* 22, 17–25. doi:10.1016/j.ecoleng.2003.11.004.
- Gallop, S.L., Bosserelle, C., Pattiaratchi, C., Eliot, I., 2011. Hydrodynamic and morphological response of a perched beach during sea breeze activity. *Journal of Coastal Research: Proceedings of the 11th International Coastal Symposium ICS 2009, Szczecin, Poland, Special Issue*, 64, pp. 75–79.
- González, M., Medina, R., Losada, M.A., 1999. Equilibrium beach profile model for perched beaches. *Coastal Engineering* 36, 343–357. doi:10.1016/S0378-3839(99)00018-6.
- Green, S., 2008. Development of conceptual models for erosion hazard assessment on a rocky embayed coast: Trigg to Sorrento, Western Australia, BSc(Hons) thesis, School of Earth and Environment, The University of Western Australia, Crawley, Western Australia, Australia.

- Hanson, H., Militello, A., 2005. Representation of nonerodible (hard) bottom in two-dimensional morphology change models, Coastal and Hydraulic Engineering Technical Note ERDC/CHL CHETN-IV-63. Army Engineer Research and Development Center, Vicksburg, Missouri.
- Hegge, B., Eliot, I.G., Hsu, J., 1996. Sheltered sandy beaches of southwestern Australia. *Journal of Coastal Research* 12 (3), 748–760.
- Johnson, D., Pattiaratchi, C., 2004. Application, modelling and validation of surfzone drifters. *Coastal Engineering* 51 (5–6), 455–471. doi:10.1016/j.coastaleng.2004.05.005.
- Kempin, G.M., 1953. Beach sand movements at Cottosloe, Western Australia. *Journal of the Royal Society of Western Australia* 37, 35–60.
- Keport, J.D., Smith, R.K., 1992. A simple model of the Australian West Coast Trough. *Monthly Weather Review* 120, 2042–2055.
- Komar, P.D., 1998. *Beach Processes and Sedimentation*, Second Ed. Prentice Hall, Upper Saddle River, New Jersey.
- Kraus, N.C., 1988. The effects of seawalls on the beach: a literature review. *Journal of Coastal Research* SI 4, 1–29.
- Kraus, N.C., McDougal, W.G., 1996. The effects of seawalls on the beach: Part 1, an updated literature review. *Journal of Coastal Research* 12 (3), 691–701.
- Larson, M., Kraus, N., 2000. Representation of non-erodible (hard) bottoms in beach profile change modeling. *Journal of Coastal Research* 16 (1), 1–14.
- Lemm, A., Hegge, B., Masselink, G., 1999. Offshore wave climate, Perth (Western Australia), 1994–96. *Marine and Freshwater Research* 50 (2), 92–102. doi:10.1071/MF98081.
- Masselink, G., 1996. Sea breeze activity and its effect on coastal processes near Perth, Western Australia. *Journal of the Royal Society of Western Australia* 79, 199–205.
- Masselink, G., Pattiaratchi, C.B., 1998a. The effect of sea breeze on beach morphology, surf zone hydrodynamics and sediment resuspension. *Marine Geology* 146, 115–135. doi:10.1016/S0025-3227(97)00121-7.
- Masselink, G., Pattiaratchi, C.B., 1998b. Morphodynamic impact of sea breeze activity on a beach with cusp morphology. *Journal of Coastal Research* 14 (2), 393–409.
- Masselink, G., Pattiaratchi, C.B., 1998c. Morphological evolution of beach cusps and associated swash circulation patterns. *Marine Geology* 146, 93–113. doi:10.1016/S0025-3227(97)00129-1.
- Masselink, G., Pattiaratchi, C.B., 2001a. Characteristics of the sea breeze system in Perth Western Australia, and its effect on the near shore wave climate. *Journal of Coastal Research* 17 (1), 173–187.
- Masselink, G., Pattiaratchi, C.B., 2001b. Seasonal changes in beach morphology along the sheltered coast of Perth, Western Australia. *Marine Geology* 172, 243–263. doi:10.1016/S0025-3227(00)00128-6.
- Muñoz-Pérez, J.J., Medina, R., 2010. Comparison of long-, medium- and short-term variations of beach profiles with and without submerged geological control. *Coastal Engineering* 57, 241–251. doi:10.1016/j.coastaleng.2009.09.011.
- Muñoz-Pérez, J.J., Tejedor, L., Medina, R., 1999. Equilibrium beach profile model for reef-protected beaches. *Journal of Coastal Research* 15 (4), 950–957.
- Murphy, P., 2011. A study of a shoreline salient formed due to a limestone reef at Yancheop Lagoon, Western Australia. Honors Dissertation, The University of Plymouth, U.K.
- Naylor, L.A., Stephenson, W.J., Trenhaile, A.S., 2010. Rock coast geomorphology: recent advances and future research directions. *Geomorphology* 114 (1–2), 3–11. doi:10.1016/j.geomorph.2009.02.004.
- Pattiaratchi, C.B., Eliot, M., 2009. Sea level variability in south-west Australia: from hours to decades, paper presented at 31st International Conference on Coastal Engineering. ASCE, Hamburg, Germany, pp. 1186–1198.
- Pattiaratchi, C., Hegge, B., Gould, J., Eliot, I., 1997. Impact of sea-breeze activity on near-shore and foreshore processes in southwestern Australia. *Continental Shelf Research* 17 (13), 1539–1560. doi:10.1016/S0278-4343(97)00016-2.
- Playford, P.E., Cope, R.N., Cockbain, A.E., Low, G.H., Lowry, D.C., 1975. Phanerozoic. *Geology of Western Australia: Mem., 2*. Geological Survey of Western Australia, Australia, pp. 223–433.
- Ranasinghe, R., Turner, I., Symonds, G., 2006. Shoreline response to submerged structures: a numerical and physical modelling study. *Coastal Engineering* 53, 589–611.
- Rey, D., Rubio, B., Bernabeu, A.M., Vilas, R., 2004. Formation, exposure, and evolution of a high-latitude beachrock in the intertidal zone of the Corrubedo complex (Ria de Arousa, Galicia, NW Spain). *Sedimentary Geology* 169, 93–105. doi:10.1016/j.sedgeo.2004.05.001.
- Roelvink, D., Reniers, A., Van Dongeren, A., Thiel, Van, de Vries, J., McCall, R., Lescinski, J., 2009. Modelling storm impacts on beaches, dunes and barrier islands. *Coastal Engineering* 56, 1133–1152.
- Sanderson, P., 2000. A comparison of reef-protected environments in Western Australia: the central west and Ningaloo coasts. *Earth Surface Processes and Landforms* 25, 397–419.
- Sanderson, P., Eliot, I.G., 1996. Shoreline salients, cusped forelands and tombolos on the coast of Western Australia. *Journal of Coastal Research* 12, 761–773.
- Sanderson, P., Eliot, I., 1999. Compartmentalisation of beachface sediments along the southwestern coast of Australia. *Marine Geology* 162 (1), 145–164.
- Searle, P., Semeniuk, V., 1985. The natural sectors of the inner Rottnest shelf coast adjoining the Swan coastal plain. *Journal of the Royal Society of Western Australia* 67 (3–4), 116–136.
- Semeniuk, V., Johnson, D.P., 1982. Recent and Pleistocene beach/dune sequences, Western Australia. *Sedimentary Geology* 32, 301–328. doi:10.1016/0037-0738(82)90042-2.
- Short, A.D., 2006. Australian beach systems—nature and distribution. *Journal of Coastal Research* 22 (1), 11–27.
- Stephenson, W.J., Thornton, L.E., 2005. Australian rock coasts: review and prospects. *Australian Geographer* 36 (1), 95–115. doi:10.1080/00049180500050946.
- Tapper, N., Hurry, L., 1993. *Australia's Weather Patterns: An Introductory Guide*. Dellasta Pty Ltd, Mount Waverly, Victoria, Australia.
- Trenhaile, A.S., 2004. Modelling the accumulation and dynamics of beaches on shore platforms. *Marine Geology* 206, 55–72. doi:10.1016/j.margeo.2004.03.013.
- Turner, R.J., 2000. Investigations on ridge and runnel topography and its influence on beach morphodynamics, paper presented at the Seventh Conference on Geology of Long Island and Metropolitan New York, Southampton, NY.
- Valvo, L., Murray, A.B., Ashton, A., 2006. How does underlying geology affect coastline change? An initial modeling investigation. *Journal of Geophysical Research* 111, F02025. doi:10.1029/2005JF000340.
- Vousdoukas, M.I., Velegrakis, A.F., Plomaritis, T.A., 2007. Beachrock occurrence, characteristics, formation mechanisms and impact. *Earth Science Reviews* 85, 23–46. doi:10.1016/j.earscirev.2007.07.002.
- Vousdoukas, M.I., Velegrakis, A.F., Karambas, T.V., 2009. Morphology and sedimentology of a microtidal beach with bedrocks: Vatera, Lesbos, NE Mediterranean. *Continental Shelf Research* 29 (16), 1937–1947. doi:10.1016/j.csr.2009.04.003.
- Walton, T.L., Sensabaugh, W., 1979. *Seawall Design on the Open Coast*, Florida Sea Grant College Rpt No. 29, Florida.